

arXiv:2502.04338v1 [physics.plasm-ph] 31 Jan 2025

IMPLEMENTATION OF AN ITER-RELEVANT QP-BASED CURRENT LIMIT AVOIDANCE ALGORITHM IN THE TCV TOKAMAK

A PREPRINT

Domenico Frattolillo

DIETI,
Università degli Studi di Napoli Federico II,
and Consorzio CREATE,
Via Claudio 21, 80125 Napoli, Italy.
domenico.frattolillo@unina.it

Adriano Mele

Swiss Plasma Center,
École Polytechnique Fédérale de Lausanne,
Rte Cantonale, 1015 Lausanne, Switzerland
adriano.mele@epfl.ch

Cristian Galperti

Swiss Plasma Center,
École Polytechnique Fédérale de Lausanne,
Rte Cantonale, 1015 Lausanne, Switzerland
cristian.galperti@epfl.ch

Luigi E. di Grazia

Consorzio CREATE,
Via Claudio 21, 80125 Napoli, Italy.
luigiemanuel.digrazia@consorziocreate.it

Massimiliano Mattei

DIETI,
Università degli Studi di Napoli Federico II,
and Consorzio CREATE,
Via Claudio 21, 80125 Napoli, Italy.
massimiliano.mattei@unina.it

Stefano Coda

Swiss Plasma Center,
École Polytechnique Fédérale de Lausanne,
Rte Cantonale, 1015 Lausanne, Switzerland
stefano.coda@epfl.ch

Gianmaria De Tommasi

DIETI,
Università degli Studi di Napoli Federico II,
and Consorzio CREATE,
Via Claudio 21, 80125 Napoli, Italy.
detommas@unina.it

Alfredo Pironti

DIETI,
Università degli Studi di Napoli Federico II,
and Consorzio CREATE,
Via Claudio 21, 80125 Napoli, Italy.
pironti@unina.it

Alessandro Tenaglia

DICII,
Università degli Studi di Roma "Tor Vergata",
Via del Politecnico, 1, 00133 Roma, Italy.
alessandro.tenaglia@uniroma2.it

Peter deVries

ITER Organization,
Route de Vinon sur Verdon, 13067
St Paul Lez Durance, France
Peter.DeVries@iter.org

Luigi Pangione

ITER Organization,
Route de Vinon sur Verdon, 13067
St Paul Lez Durance, France
Luigi.Pangione@iter.org

Luca Zabeo

ITER Organization,
Route de Vinon sur Verdon, 13067
St Paul Lez Durance, France
Luca.Zabeo@iter.org

TCV team

See author list of B. P. Duval et al.
2024 Nucl. Fusion 64 112023

Eurofusion Tokamak Exploitation Team

See author list of E. Joffrin et al.
2024 Nucl. Fusion 64 112019

February 10, 2025

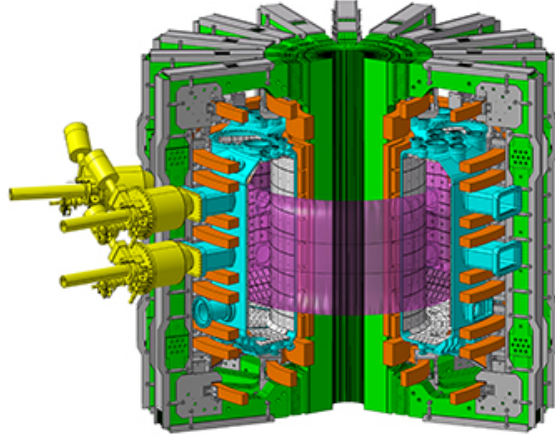


Figure 1: Cutaway view of the TCV tokamak, showing the PF coils (orange), the TF coils (green), the vacuum vessel (cyan), and the plasma region (purple). In addition, some of the ECRH launchers installed on TCV are also displayed in yellow.

ABSTRACT

The problem of avoiding saturation of the coil currents is critical in large tokamaks with superconducting coils like ITER. Indeed, if the current limits are reached, a loss of control of the plasma may lead to a major disruption. Therefore, a Current Limit Avoidance (CLA) system is essential to operate safely. This paper provides the first experimental evidence that the online solution of a constrained quadratic optimization problem can offer a valid methodology to implement a CLA. Experiments are carried out on the Tokamak à Configuration Variable (TCV) at the Swiss Plasma Center, showing the effectiveness of the proposed approach and its suitability for real-time application in view of future reactors such as ITER.

Keywords Current limit avoidance · Input allocation · Plasma magnetic control · Tokamaks

1 Introduction

The tokamak concept is still considered a baseline for designing a potential power plant reactor based on thermonuclear fusion [1]. The next step in this direction is the International Thermonuclear Experimental Reactor (ITER) [2], which will extensively test concepts and technologies required for the design and construction of a fusion reactor. A tokamak is a toroidal-shaped device in which a fully ionized gas of hydrogen isotopes is heated up to temperatures of hundreds of millions of degrees Celsius, where the thermal agitation of the electrically charged nuclei can overcome the Coulomb repulsive force. This makes possible collisions producing fusion reactions. External magnetic fields allow the confinement of such a hot plasma. These fields are generated using currents flowing in the Poloidal Field (PF) and the Toroidal Field (TF) coils. These are shown in a simplified schematic for the TCV tokamak in Fig. 1.

An important role in tokamaks is played by magnetic control which is needed since day one and is essential to successfully control high-performance plasmas, such as those envisaged for ITER [3].

Controlling the current induced in the plasma, as well as the plasma shape and position [4] are all problems relying on the currents flowing in the PF circuits as actuators [5]. Robust control design techniques have been proposed in the literature [6–9] aiming to reject unexpected disturbances and cope with model uncertainties. In practice however, any plasma magnetic control algorithm requires that PF coil currents are sufficiently far from their limits, in order to allow for reasonable margins to react to unexpected events. Open-loop strategies for the optimization of the nominal PF current waveforms can be adopted [10–13]. However, these may not be effective at the highest values of the plasma current or in the presence of unexpected disturbances [14].

As a consequence, it is important for a reliable plasma magnetic control system to include a Current Limit Avoidance (CLA) system to safely operate the machine also when disturbances and/or uncertainties drive the PF currents close to their limits [15–17]. In fact, for a critical infrastructure such as a nuclear power plant, common-mode failures must be avoided by adopting different hardware and software solutions. In [18], three different limit avoidance algorithms are described.

Other possible approaches to limit currents in the active circuits resemble Model Predictive Control (MPC, [7, 19]). However, while the implementation of a MPC scheme typically needs the knowledge of the plant dynamics, this is not the case for the CLA approach, provided that a so-called current control scheme is adopted [5]. In addition, optimization problems arising in MPC control schemes are usually larger than those solved in the CLA formulation proposed in this article, as they must take into account more than one prediction step. This makes the CLA architecture less demanding from a computational point of view.

The CLA strategy has proven its effectiveness in numerical simulations on the DEMO device [18, 20], and has been proposed for inclusion in the ITER Plasma Control System (PCS) [21]. In this paper, the current limit avoidance system proposed for ITER is tested as a proof of concept on TCV, a medium-sized tokamak operated by the Swiss Plasma Center of the École Polytechnique Fédérale de Lausanne. The flexibility of TCV’s upgraded Distributed Control System (Système de Contrôle Distribué, or SCD [22]) enables rapid and effective implementation and testing of novel plasma control solutions, including a recently implemented shape control algorithm [23, 24] and an alternative version of the CLA system which relies on a combination of a dynamic optimizer and a static annihilator [25]. The significantly faster dynamics observed in TCV plasmas with respect to the ones expected in larger devices such as ITER require higher sampling frequencies in the control system, making the real-time implementation more challenging; this in turn implies that solutions adopted on TCV are expected to be easily scalable to future reactors, at least from the computational point of view, making TCV an ideal testbed for tokamak control technologies. One of the main differences between ITER and TCV is in the technology of the coils. TCV is not a superconductive tokamak, which means that resistive copper coils are used to confine the plasma, while for ITER a set of superconductive coils is foreseen. However, the proposed CLA system only uses steady-state information, allowing for a proper validation of the proposed methodology despite the difference in the coil dynamics between the TCV and ITER devices.

The rest of this paper is organized as follows. Section 2 briefly describes the TCV tokamak and its PCS; Section 3 introduces the CLA methodology; in Section 4, experimental results are given; finally, Section 5 concludes the article.

2 TCV magnetic control system

A layout of the TCV poloidal cross-section is shown in Fig. 2. The core magnetic controller in the TCV digital control system is designed to emulate the legacy analog system, called the *hybrid* controller. The name comes from the fact that the original system was a hybrid digital-analog controller, where the computations were carried out analogically, but the gain matrices could be switched digitally. The hybrid controller, represented as the orange block in Fig. 3, is a Multiple-Input Multiple-Output (MIMO) controller that takes care of the vertical stabilization of the plasma and of the regulation of the plasma current I_p , of the radial and vertical plasma centroid displacement, and of tracking scenario coil currents. In particular, the average current in the *OH* coils and two combinations of the *EF* ones are dedicated to I_p control and to plasma position control, respectively. The remaining currents are projected in a space that is orthogonal to these combinations; for details, see [24]). The hybrid controller generates voltage requests for the PF coils, which are summed to feedforward traces V_{ff} , computed offline, to obtain the voltage requests V_a to the coil power supplies.

Notice that, to be able to stabilize the plasma vertically, the digital version of this controller needs to run at a rather high sampling rate, typically chosen equal to 10 kHz.

As it is common in many tokamaks, the controller relies on magnetic and current measurements to reconstruct plasma position and current. In addition, a fast observer of the vertical position is obtained by using the in-vessel magnetic probes only, which are less affected by the shielding effect of the passive structures, and this is used by the vertical stabilization control loop.

The hybrid controller also includes a channel to control the plasma density, reconstructed through interferometry, which in practice is completely decoupled from the magnetic controller. A detailed analysis of the hybrid controller is given in [24]. An emulator of this controller is available in Matlab-Simulink, allowing to simulate the behavior of the controller before its real-time application. Moreover, the framework allows for automatic code generation and deployment of control algorithms directly in the SCD system [26], providing a friendly environment to extend the capabilities of the original controller.

Furthermore, the TCV magnetic control system is equipped with a plasma shape controller, as shown in Fig. 3; the design and validation of such controller are extensively discussed in [23, 24]. Unlike the hybrid controller, the feedback

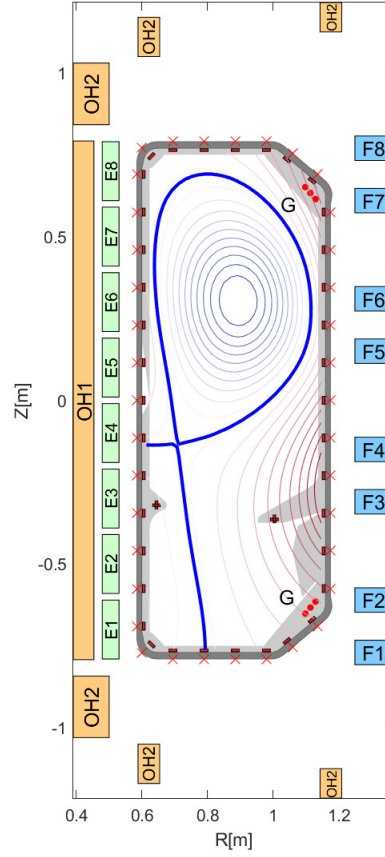


Figure 2: TCV poloidal cross-section (taken from [23]).

signals for the shape controller, which is based on the *isoflux* approach and modifies the reference signals of the hybrid block, are obtained by interpolating the poloidal flux and magnetic field maps obtained from the real-time equilibrium reconstruction code LIUQE [27]. In practice, the necessity of a full equilibrium reconstruction limits the sampling rate of the shape controller to 1 kHz.

Finally, note that the coils used for plasma shaping in TCV are the sets E1-8 and F1-8 shown in Fig. 2 in red and blue, respectively. Therefore, the associated currents I_{EF} are the ones that will be considered in the allocation problem solved by the CLA.

3 The Current Limit Avoidance Algorithm

The proposed CLA system, shown in blue in Fig. 3, acts in parallel to the shape controller, providing additional control actions, summed to the hybrid controller reference signals r_h with the aim of optimizing a quadratic cost function while simultaneously satisfying a set of hard linear constraints. Moreover, the steady-state effect of the allocator on the plasma shape is subtracted from the reference signals r_{sh} , to avoid any conflict between the two systems. The objective of the proposed CLA system is to reduce any excess of currents with respect to saturation limits by resorting to an alternative control pattern that allows the re-allocation of the currents while minimizing the degradation in terms of the shape control performance.

The CLA receives as input the references r_h to the hybrid controller, modified by the action of the shape controller u_{sh} . As discussed in Section 1, the proposed allocator acts based on the steady-state effect of the shape control inputs on the coil currents. For this reason, the first step is to obtain an estimate of their steady-state value. To do so, the

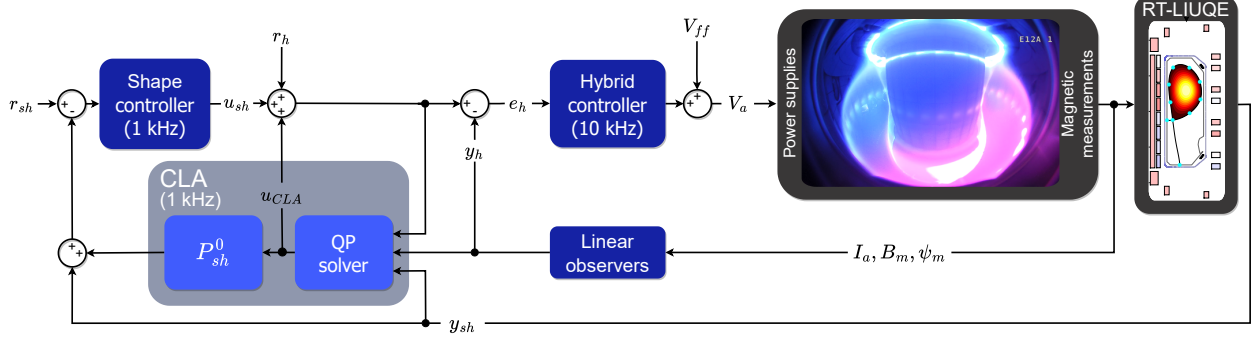


Figure 3: TCV control scheme: in orange the hybrid magnetic controller, including a control loop for the PF currents; in green the shape controller; in blue the proposed CLA system.

proposed CLA system takes into account the static gain of the closed-loop system consisting of the linearized TCV plasma response in the vicinity of the considered plasma configuration and a state-space model of the hybrid controller. Let us denote the static gain from (variations of) the hybrid control error e_h to the currents in the E and F coils of TCV as P_{EF}^0 and the gain from e_h to variations in the plasma shape descriptors y_{sh} as P_{sh}^0 . Then, assuming that the plasma is close to the desired scenario configuration and denoting with y_h the outputs of the plant controlled by the hybrid loop, an estimate of the steady-state value of the currents in the E and F coils of TCV can be obtained at each controller step as

$$I_{EF}^0 = \underbrace{I_{EF}}_{\text{measured currents}} + \underbrace{P_{EF}^0(u_{sh} + r_h - y_h)}_{\text{expected variation at steady-state}}. \quad (1)$$

Similarly, the steady-state effect of the CLA on the plasma shape descriptors y_{sh} can be estimated as

$$\delta y_{sh}^0 = P_{sh}^0 u_{CLA}, \quad (2)$$

while the steady-state effect of the CLA only on the I_{EF} currents is

$$\delta I_{EF}^0 = P_{EF}^0 u_{CLA}. \quad (3)$$

At every time step, the CLA solves the following Quadratic Programming (QP) optimization problem

$$\min_{u_{CLA}} \quad \delta y_{sh}^{0T} W \delta y_{sh}^0 + \delta I_{EF}^{0T} Q \delta I_{EF}^0, \quad (4)$$

$$\text{s.t.} \quad \underline{I}_{EF} \leq I_{EF}^0 \leq \bar{I}_{EF} \quad (5)$$

where \underline{I}_{EF} and \bar{I}_{EF} represent the lower and upper bounds on the EF coil currents, respectively. The first term of the cost function aims at minimizing the effect of the CLA on the shape descriptors y_{sh} , while the second aims at reducing its effect on the PF coil currents. Hence, if the steady-state current vector I_{EF}^0 satisfies the constraints of the optimization problem, the optimal solution is given by $u_{CLA} = 0$, i.e., the CLA leaves the references to the hybrid controller r_h unmodified.¹

On the other hand, since the current saturations are specified as hard inequality constraints, if some of the currents in the vector I_{EF}^0 exceed the limit, then the CLA will provide a nonzero correction u_{CLA} to the requests r_h given to the hybrid controller, to bring all currents back to the safe region while minimizing at the same time the effect on the plasma shape. In addition, as shown in Fig. 3, a term $P_{sh}^0 u_{CLA}$ is subtracted from the reference signals r_{sh} , in order to hide the effect of the allocator at steady state from the point of view of the shape controller. In this way, the outer shape control loop will not react to the changes made by the CLA.

An important remark is that in the case of TCV and differently to what has been discussed in Section 1, the design of the CLA still (loosely) depends on the knowledge of the structure of the hybrid controller, and in particular of its

¹Alternatively, the operator may decide to minimize the I_{EF} steady-state current norm by changing the second term in the optimization to $I_{EF}^{0T} Q I_{EF}^0$, similarly to what is proposed in [25]. In this case, typically a relatively low weight Q is assigned to the current term with respect to the weight W assigned to the shape variations, and the optimizer will attempt to rearrange the currents in order to obtain a comparable shape accuracy while minimizing the weighted current norm as a secondary objective.

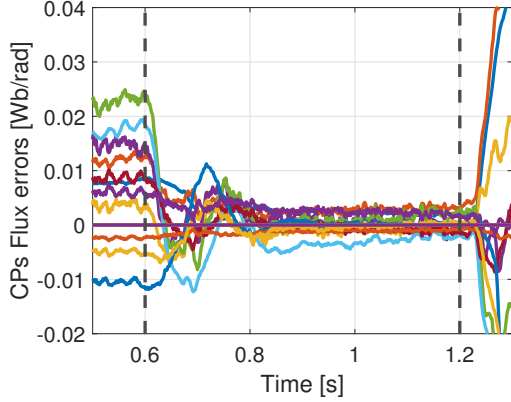


Figure 4: Reference scenario - time traces of the isoflux control errors. The beginning and end of the controlled time window are indicated by the dashed black lines.

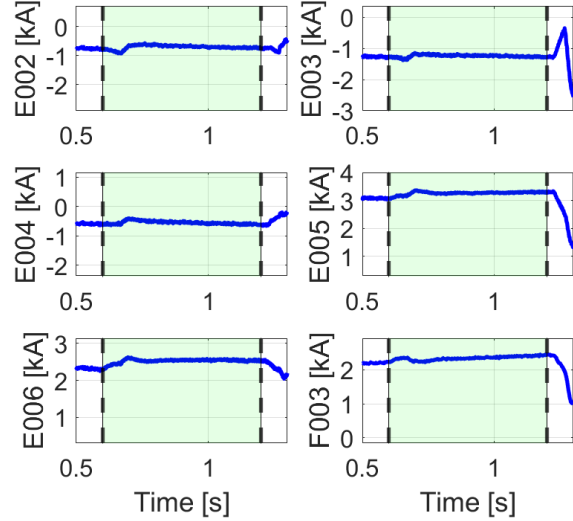


Figure 5: Reference scenario - time traces for some of the currents in the E and F coils.

steady-state gain. This is due to the fact that, in TCV, the control of the coil currents and the plasma current and position is tightly coupled, while the shape control also generates reference variations for the plasma position channels. On the other hand, in other tokamak magnetic control architectures, where the plasma position and I_p controllers generate references for an internal loop that regulates the currents in the PF coils, this knowledge is not necessary under the assumption that the coil current controller has an approximately unitary steady-state gain on all channels, i.e., that the steady-state values of the PF currents are close to the respective references. This is, for example, the case of the foreseen ITER control system.

Finally, notice that, in other formulations of the same problem (such as [18]), the effect of the CLA on the plasma current is also taken into account explicitly through an additional term in the optimization cost function. However, in TCV the I_p control is achieved by a dedicated set of coils (OH1-2 in Fig. 2) on time scales that are significantly faster than those of the shape control, so this term can be neglected in the case under exam.

4 Experimental results

The effectiveness of the proposed CLA approach is demonstrated in three different test cases on a TCV lower single-null reference scenario, shown in Fig. 2:

- **Test case I:** the limit on one circuit is fictitiously reduced.
- **Test case II:** the limits on three circuits are fictitiously reduced.
- **Test case III:** the limit on one circuit is fictitiously reduced in a time-varying fashion.

The reference scenario, taken from TCV pulse #79742, is a $I_p = 250$ kA lower single null plasma. The isoflux shape control described in [24] is activated during the flat top phase from 0.6 s to 1.2 s. Fig. 4 shows the time behavior of the shape control errors in the case where no saturation limit is acting on the PF currents. Fig. 5 shows the currents in some circuits of interest for the considered test cases.

The real-time implementation of the CLA system relies on the availability of an effective solver for the QP problem (4). The implementation proposed for this work is based on the C++ library [28], which implements the Goldfarb-Idnani active-set dual method [29]. As it can be seen from figs.10-15-20, the solver converged within 3 iterations for all the considered cases, even when multiple current saturations were hit simultaneously.

4.1 Test Case I

The first of the proposed tests was performed in TCV shot #83435, and the results are reported in figs. 6-9. The shape control error traces are shown in Fig. 7, where a degradation of the control performance can be observed with respect to

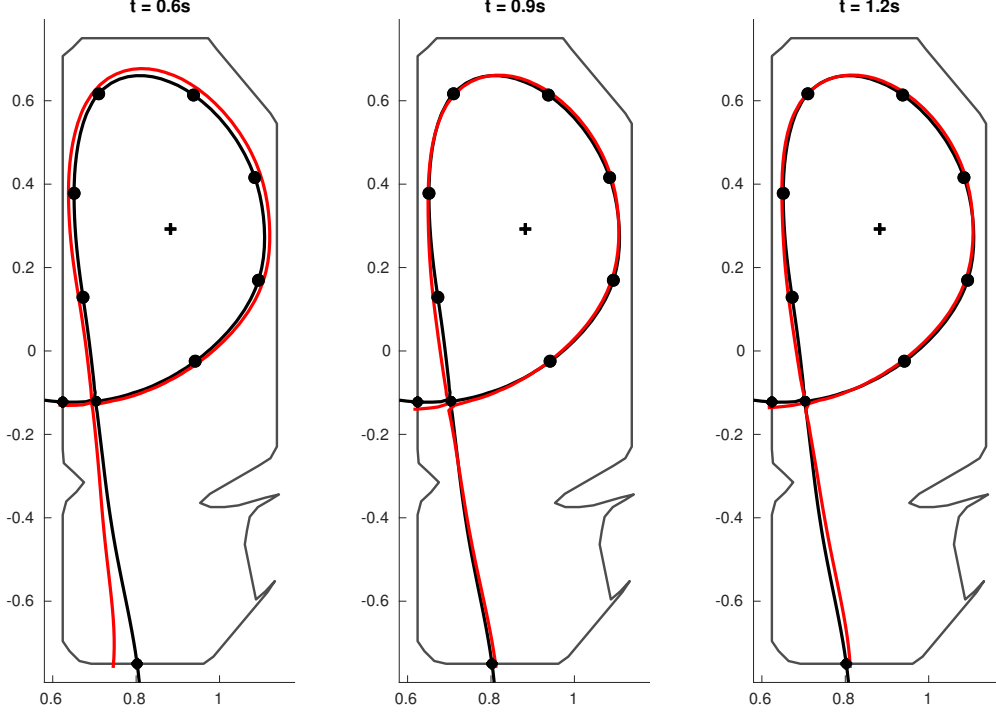


Figure 6: Test Case I - snapshots at different time instants. The experimental plasma separatrix is shown in red, while the boundary for the reference target equilibrium is shown in black. The black dots are the considered isoflux control points.

the baseline case in Fig. 4. On the other hand, Fig. 6 shows the snapshots at three time instants of interest, from which it can be seen that the degradation in plasma shape control performance introduced by the CLA action is almost negligible at steady-state from the practical point of view. The coil currents that are closest to saturation and the corresponding saturation limits are also reported in Fig. 8, where it can be seen how the $E5$ current returns into an acceptable band following the activation of the CLA at $t = 0.6s$. The QP cost function is reported in Fig. 9, while the iterations needed by the QP solver are shown in Fig. 10.

4.2 Test Case II

The results for the second test case, performed in TCV shot #83437, are reported in Figs. 11-14. The snapshots at three different time instants in Fig. 11 illustrate the plasma shape degradation due to the CLA contribution; it can be observed how, in this case, the performance degradation is more evident in the region close to the X-point and the inner strike point. Fig. 12 displays the time traces of the shape control errors. The relevant coil currents and corresponding saturation limits are reported in Fig. 13, where it can be seen how the $E5$ current is brought back into an acceptable band after the activation of the CLA at $t = 0.6s$; to compensate, the $E6$ current moves closer to its saturation, also artificially reduced to 2.5 kA. The QP cost function is reported in Fig. 14, with the iterations needed by the QP solver shown in Fig. 15.

4.3 Test Case III

The results for the third test case, TCV shot #83438, are reported in figs. 16-19. For this case, the saturation on the $E5$ coils decreases in steps of 250 A applied every 0.2 s. The snapshots at three different time instants following the CLA activation are shown in Fig. 16, while the time traces of the shape control errors are shown in Fig. 17. The shape accuracy degradation is comparable to the one observed in test case II, but in this case the time-varying nature of the saturation limit is clearly reflected by the small jumps observed in the shape control error traces in Fig. 17 and in the behavior of the QP cost function, reported in Fig. 19. The relevant coil currents and corresponding saturation limits are reported in Fig. 18, where the variable saturation limit for the $E5$ current is also shown. The $E5$ current returns into the acceptable time-varying band following the activation of the CLA at $t = 0.6$. The iterations performed by the QP solver are shown in Fig. 20.

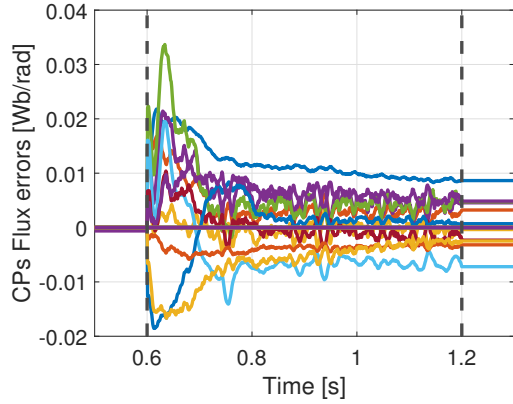


Figure 7: Test Case I - time traces of the isoflux control errors. The beginning and end of the controlled time window are indicated by the dashed black lines.

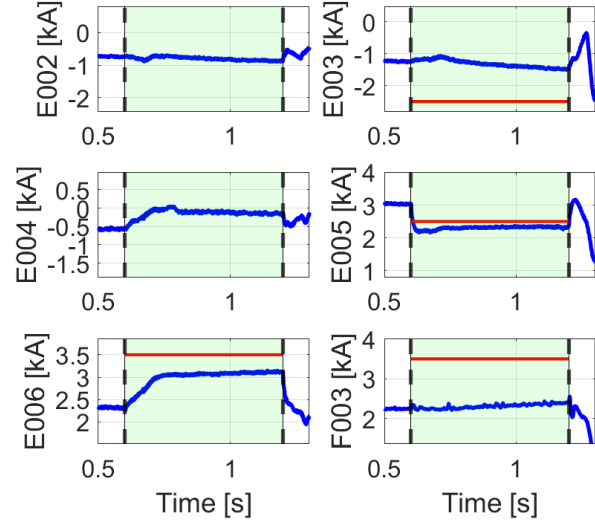


Figure 8: Test Case I - time traces of the PF currents (blue) compared with saturation limits (red).

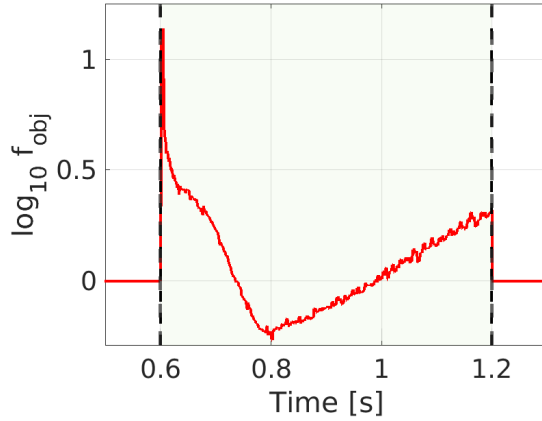


Figure 9: Test Case I - time trace of the QP problem objective function.

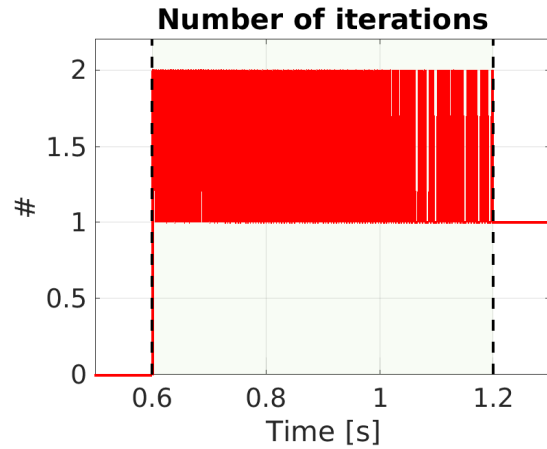


Figure 10: Test Case I - iterations performed by the QP solver.

5 Conclusive Remarks

This paper describes the implementation of an effective solution to tackle the problem of the PF currents saturation. The methodology proposed for inclusion in the ITER PCS has been tested experimentally on the TCV tokamak. The algorithm proved to be capable of dealing robustly with the saturation of several active circuit currents, up to four in Test Case II, and also proved to be capable of handling time-varying saturations, as demonstrated in Test Case III. The simplicity of the proposed scheme and the tractable computation cost make this algorithm an effective tool for future reactors such as ITER.

Acknowledgments

This work has been supported by the following financial contributions:

- Grant Agreement No 101052200 — EUROfusion and training programme 2014-2018 and 2019-2020 under grant agreement No. 633053.

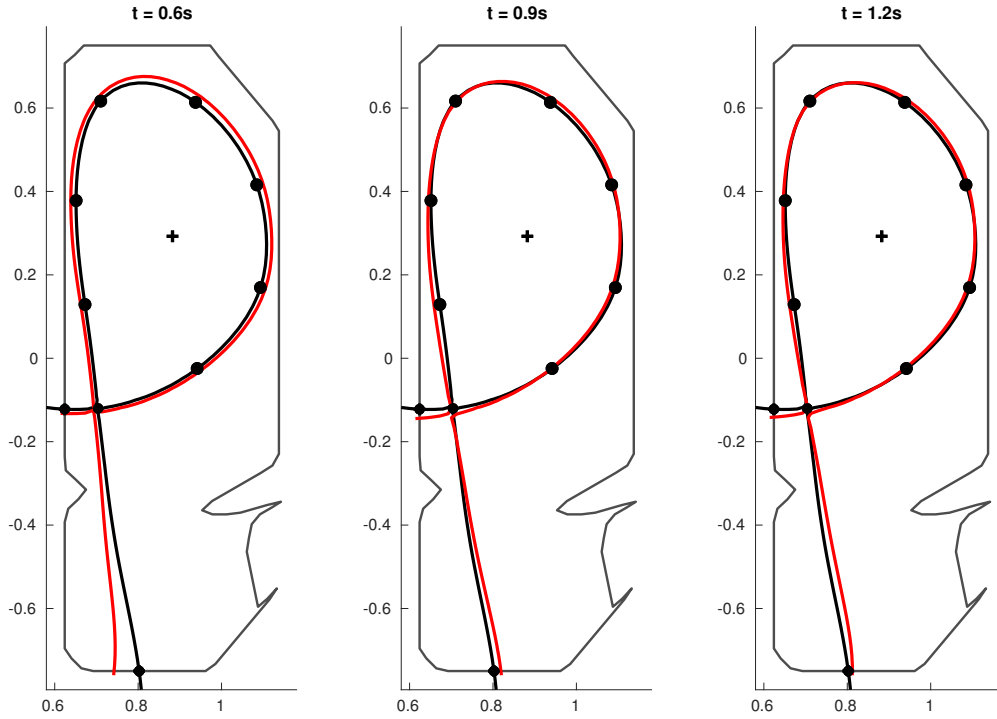


Figure 11: Test Case II - snapshots at different time instants. The experimental plasma separatrix is shown in red, while the boundary for the reference target equilibrium is shown in black. The black dots are the considered isoflux control points.

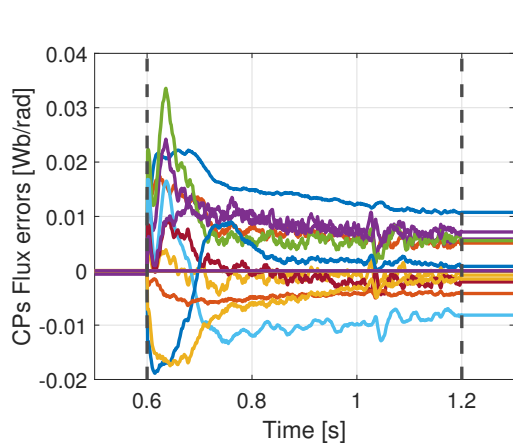


Figure 12: Test Case II - time traces of the isoflux control errors. The beginning and end of the controlled time window are indicated by the dashed black lines.

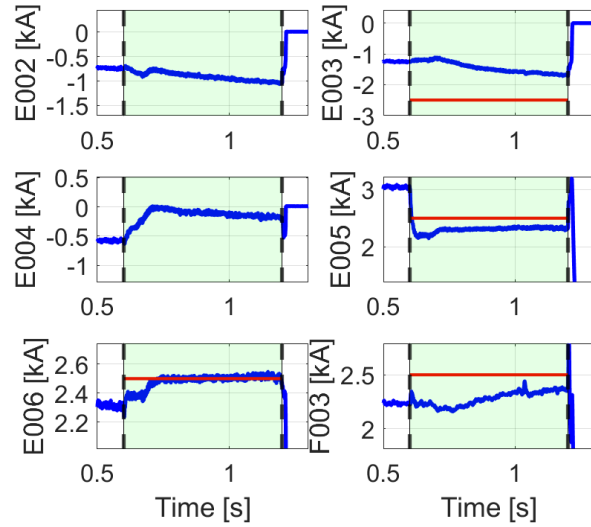


Figure 13: Test Case II - time traces of the PF currents (blue) compared with saturation limits (red).

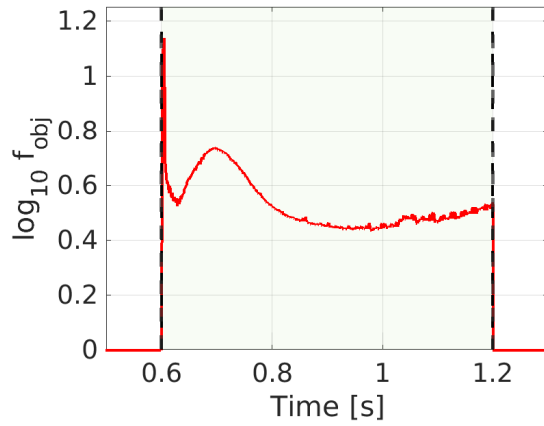


Figure 14: Test Case II - time trace of the QP problem objective function.

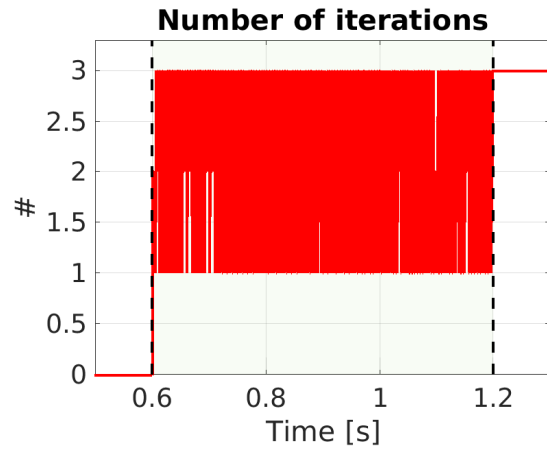


Figure 15: Test Case II - iterations performed by the QP solver.

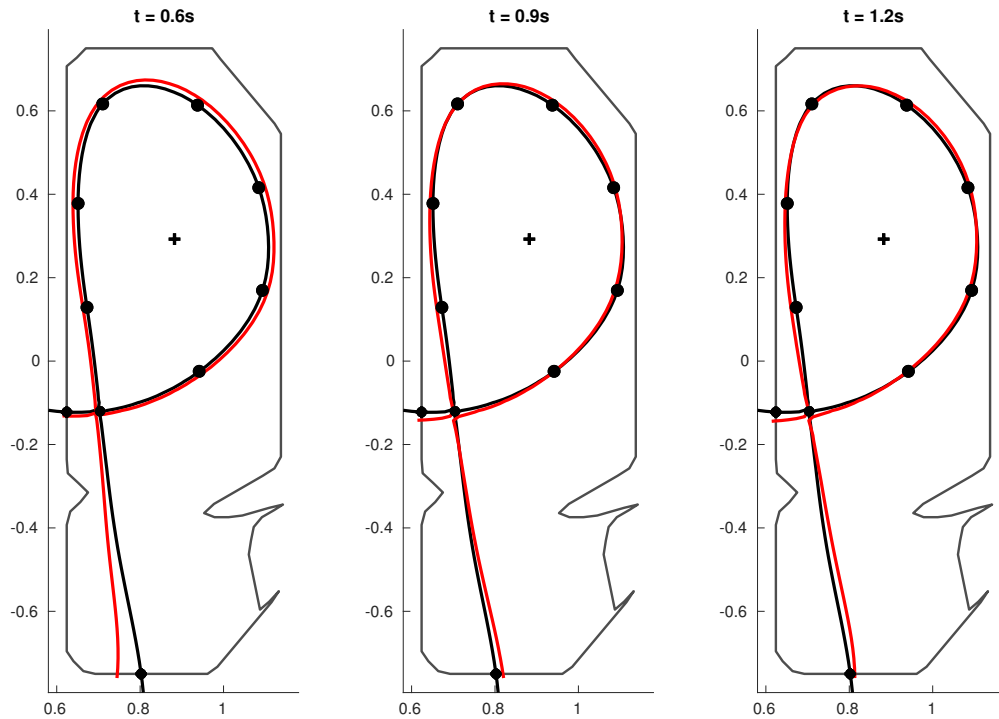


Figure 16: Test Case III - snapshots at different time instants. The experimental plasma separatrix is shown in red, while the boundary for the reference target equilibrium is shown in black. The black dots are the considered isoflux control points.

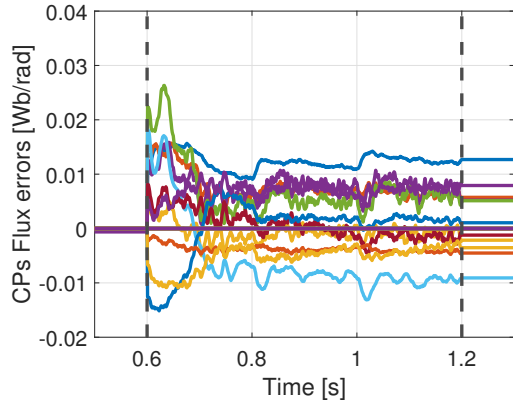


Figure 17: Test Case III - time traces of the isoflux control errors. The beginning and end of the controlled time window are indicated by the dashed black lines.

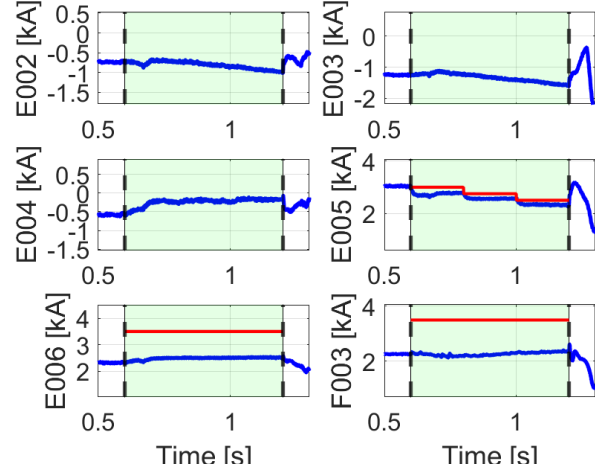


Figure 18: Test Case III - time traces of the PF currents (blue) compared with saturation limits (red).

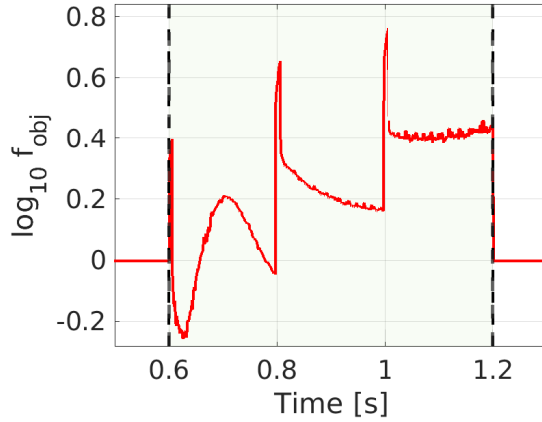


Figure 19: Test Case III - time trace of the QP problem objective function.

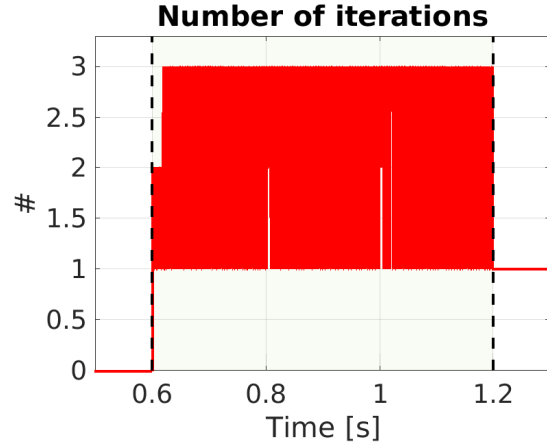


Figure 20: Test Case III -iterations performed by the QP solver.

- Swiss State Secretariat for Education, Research and Innovation (SERI).
- TRAINER project (CUP E53D23014670001) funded by EU in NextGenerationEU plan through the Italian “Bando Prin 2022 - D.D. 1409 del 14-09-2022” by MUR
- Italian Research Ministry under project PRIN 2022JCZJ33.

Opinions expressed are those of the author(s) only and do not necessarily reflect those of the European Union (EU), the European Commission (EC), ITER IO, or SERI. Neither the EU nor the EC nor SERI can be held responsible for them.

References

- [1] Wesson, J., Campbell, D.J.: Tokamaks, vol. 149. Oxford University Press (2011)
- [2] ITER Organization: ITER. URL <https://www.iter.org/>
- [3] Snipes, J.A., et al.: ITER plasma control system final design and preparation for first plasma. Nucl. Fusion **61**(10), 106,036 (2021). doi:<https://doi.org/10.1088/1741-4326/ac2339>
- [4] Ariola, M., Pironi, A.: Magnetic Control of Tokamak Plasmas, 2nd edn. Springer (2016)

- [5] De Tommasi, G.: Plasma magnetic control in tokamak devices. *J. Fusion Energy* **38**(3-4), 406–436 (2019). doi:<https://doi.org/10.1007/s10894-018-0162-5>
- [6] Ariola, M., Ambrosino, G., Pironti, A., Lister, J.B., Vyas, P.: Design and experimental testing of a robust multivariable controller on a tokamak. *IEEE Trans. Control. Syst. Technol.* **10**(5), 646–653 (2002). doi:<https://doi.org/10.1109/tcst.2002.801805>
- [7] Mattei, M., Labate, C.V., Famularo, D.: A constrained control strategy for the shape control in thermonuclear fusion tokamaks. *Automatica* **49**(1), 169–177 (2013). doi:<https://doi.org/10.1016/j.automatica.2012.09.004>
- [8] Gerkšič, S., Pregelj, B., Perne, M., Ariola, M., De Tommasi, G., Pironti, A.: Model predictive control of ITER plasma current and shape using singular-value decomposition. *Fusion Eng. Des.* **129**, 158–163 (2018). doi:<https://doi.org/10.1016/j.fusengdes.2018.01.074>
- [9] Wai, J.T., Vail, P.J., Kolemen, E.: Control pathway for an advanced divertor on ITER. *Fusion Eng. Des.* **159**, 111,957 (2020). doi:<https://doi.org/10.1016/j.fusengdes.2020.111957>
- [10] di Grazia, L., Mattei, M.: A numerical tool to optimize voltage waveforms for plasma breakdown and early ramp-up in the presence of constraints. *Fusion Eng. Des.* **176**, 113,027 (2022). doi:<https://doi.org/10.1016/j.fusengdes.2022.113027>
- [11] Mattei, M., Albanese, R., Ambrosino, G., Portone, A.: Open loop control strategies for plasma scenarios: linear and nonlinear techniques for configuration transitions. In: *Proceedings of the 45th IEEE Conference on Decision and Control*, pp. 2220–2225. IEEE (2006). doi:<https://doi.org/10.1109/cdc.2006.377412>
- [12] Luo, Z.P., Huang, Y., Yuan, Q.P., Xiao, B.J.: Fast scenario design for alternative magnetic diverted discharge on EAST. *Fusion Eng. Des.* **157**, 111,816 (2020). doi:<https://doi.org/10.1016/j.fusengdes.2020.111816>
- [13] di Grazia, L.E., Felici, F., Mattei, M., Merle, A., Molina, P., Galperti, C., Coda, S., Duval, B., Maier, A., Mele, A., et al.: Automated shot-to-shot optimization of the plasma start-up scenario in the tcv tokamak. *Nuclear Fusion* **64**(9), 096,032 (2024)
- [14] De Tommasi, G., Ambrosino, G., Ariola, M., Calabro, G., Galeani, S., Maviglia, F., Pironti, A., Rimini, F.G., Sips, A.C., Varano, G., Vitelli, R., Zaccarian, L.: Shape control with the eXtreme Shape Controller during plasma current ramp-up and ramp-down at the JET tokamak. *J. Fusion Energy* **33**, 149–157 (2014). doi:<https://doi.org/10.1007/s10894-013-9652-7>
- [15] Ambrosino, G., Ariola, M., Pironti, A., Portone, A., Walker, M.: A control scheme to deal with coil current saturation in a Tokamak. *IEEE Trans. Control. Syst. Technol.* **9**(6), 831–838 (2001). doi:<https://doi.org/10.1109/87.960346>
- [16] Varano, G., Ambrosino, G., Tommasi, G., Galeani, S., Pironti, A., Zaccarian, L.: Performance assessment of a dynamic current allocator for the JET eXtreme Shape Controller. *Fusion Eng. Des.* **86**(6-8), 1057–1060 (2011). doi:<https://doi.org/10.1016/j.fusengdes.2011.03.068>. *Proceedings of the 26th Symposium of Fusion Technology (SOFT-26)*
- [17] Boncagni, L., Galeani, S., Granucci, G., Varano, G., Vitale, V., Zaccarian, L.: Plasma position and elongation regulation at FTU using dynamic input allocation. *IEEE Trans. Control. Syst. Technol.* **20**(3), 641–651 (2012). doi:<https://doi.org/10.1109/tcst.2011.2140398>
- [18] di Grazia, L.E., Frattolillo, D., De Tommasi, G., Mattei, M.: Current Limit Avoidance Algorithms for DEMO Operation. *Journal of Optimization Theory and Applications* **198**(3), 958–987 (2023)
- [19] Camacho, E.F., Alba, C.B.: *Model predictive control*. Springer (2013)
- [20] Donné, A.: The european roadmap towards fusion electricity. *Philosophical Transactions of the Royal Society A* **377**(2141), 20170,432 (2019)
- [21] de Vries, P., et al: Strategy to systematically design and deploy the iter plasma control system: A system engineering and model-based design approach. *Fusion Engineering and Design* **204**, 114,464 (2024). doi:<https://doi.org/10.1016/j.fusengdes.2024.114464>. URL <https://www.sciencedirect.com/science/article/pii/S092037962400317X>
- [22] Galperti, C., Felici, F., Vu, T., Sauter, O., Carpanese, F., Kong, M., Marceca, G., Merle, A., Pau, A., Perek, A., et al.: Overview of the tcv digital real-time plasma control system and its applications. *Fusion Engineering and Design* **208**, 114,640 (2024)
- [23] Mele, A., Tenaglia, A., Carnevale, D., Coda, S., Felici, F., Galperti, C., Merle, A., Pironti, A., Sauter, O., the TCV team, the Tokamak Exploitation team: Design of a novel plasma shape controller for the TCV tokamak. In: *2024 10th International Conference on Control, Decision and Information Technologies (CoDIT24)*. IEEE (2024)

- [24] A. Mele, A.T.e.a.: A model-based reference governor for the control of the plasma shape in the tcv tokamak. Social Science Research Network (preprint) (2024). doi:10.2139/ssrn.5015300
- [25] Tenaglia, A., Masocco, R., Mele, A., et al.: Dynamic steady-state coil current allocation for plasma shape control: a study on the TCV tokamak. In: 10th International Conference on Control, Decision and Information Technologies. IEEE (2024)
- [26] Felici, F., Le, H., Paley, J., Duval, B., Coda, S., Moret, J.M., Bortolon, A., Federspiel, L., Goodman, T., Hommen, G., et al.: Development of real-time plasma analysis and control algorithms for the tcv tokamak using simulink. Fusion Engineering and Design **89**(3), 165–176 (2014)
- [27] Moret, J., et al.: Tokamak equilibrium reconstruction code LIUQE and its real time implementation. Fusion Engineering and Design **91**, 1–15 (2015)
- [28] Luca di Gaspero: QuadProg++. <https://github.com/liuq/QuadProgpp> (2007-2016)
- [29] Goldfarb, D., Idnani, A.: A numerically stable dual method for solving strictly convex quadratic programs. Mathematical programming **27**(1), 1–33 (1983)